

SHOCK WAVE/BOUNDARY LAYER INTERACTION

J. Müller, R. Mümmler, W. Staudacher
University of the German Armed Forces – Trisonic Windtunnel Munich

Keywords: *Shock / boundary layer / separation / supersonic / laser Doppler anemometer*

Abstract

Experiments based on laser Doppler anemometry (LDA) were performed to investigate shock/boundary layer interaction in the presence of separation. Applicability and limits of this experimental method are briefly discussed. Experiments are concentrated on flow conditions given by $M = 2.5/Re = 29 \cdot 10^6 m^{-1}$, interaction is generated by an unswept, 2-d flat plate/24 degree ramp configuration. Time averaged locations of separation, reattachment and the mean shock position are determined by measurements in closest proximity to the surfaces. Results are compared with data from pressure measurements given in literature.

1 Introduction

The fluctuating shock/boundary layer interaction significantly affects the aerodynamic characteristics in supersonic flow, especially when separation is present. To demonstrate these basic effects experimentally an unswept, two dimensional ramp is frequently used. Despite of the 2-d set up the generated flow will be rather three dimensional, especially true for close proximity to the surfaces of the model and the limiting wind tunnel walls. With growing extension of separation the degree of three dimensionality will increase.

Extensive experimental work [1], [12], [8], [9] shows, that the three dimensionality in the wall shear stress field has only minor effects on the pressure fluctuations near separation. It was found that the time averaged flow field can be regarded as essentially two dimensional.

A sketch of a two dimensional separation is shown in Fig. 1. The interaction starts at point

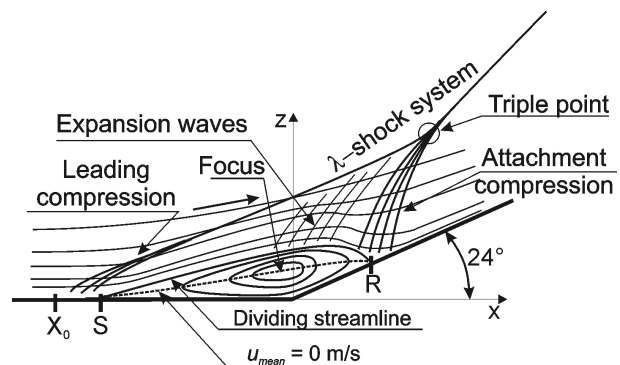


Fig. 1 Two-dimensional separation at an unswept ramp shock/boundary layer interaction

X_0 , defined as the position where the wall pressure starts to increase above the undisturbed level. Hence it is located upstream of the position of separation S.

In this region the wall pressures are unsteady [1], composed of the higher frequency, low amplitude signal of the undisturbed boundary layer and the low frequency, large amplitude signal caused by the shock. Downstream of X_0 , the shock induced effects are dominant. In any case no evidence for periodicity was ever found.

A salient indicator for the presence of the shock between X_0 and S is a local maximum of the standard deviation of the wall pressures, the maximum observed [3] being approximately 10%-30% of the local wall pressure.

The intermittence of the shock system can also be shown by taking schlieren photographs with very short exposure time [13], [10]. When comparing a sequence of pictures each photo shows an individual shock pattern.

The three dimensional separation is characterized by a significant spanwise mass flow.

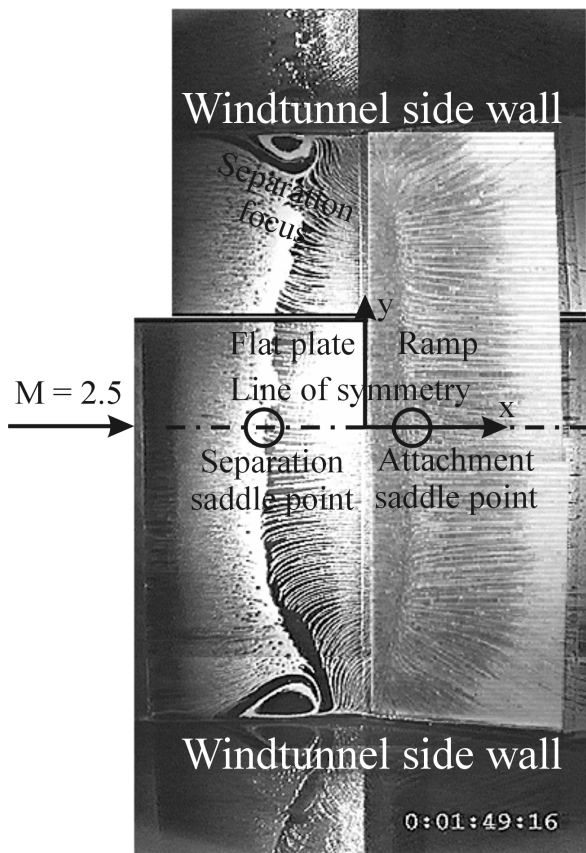


Fig. 2 Oil flow pattern at a flat plate/24-degree ramp configuration, $M=2.5$, $Re = 29 \cdot 10^6 m^{-1}$

Hence the points of separation and reattachment now cannot be connected by a dividing streamline.

Fig. 2 shows oil streak patterns ($M = 2.5$, $Re = 29 \cdot 10^6 m^{-1}$) indicating a relatively good symmetry of the flow field. The saddle point of separation is at the intersection of the line of symmetry and the separation line. The three dimensionality of the flow is emphasized by the two foci of separation close to the tunnel walls. Increasing the Mach number improves the symmetry of flow, while the streamwise extension of the bubble decreases.

The same tendency can be observed with increasing Reynolds numbers, yet the influence is significantly smaller. As described in [1] this behavior is representative only for high Reynolds numbers. A trend reversal is reported at $Re_{\delta_0} \approx 10^5$, based on the boundary layer thickness ($Re \approx 13 \cdot 10^6 m^{-1}$ here).

2 Experimental setup

2.1 Wind tunnel

The experiments were carried out in the $300 \times 675 \text{ mm}^2$ test section of the blow down type Trisonic Windtunnel Munich (TWM). The variable design of laval nozzle and diffuser gives a Mach number range between 0.3 and 3.0. For the present investigations test conditions are $M = 2.5$, $Re = 29 \cdot 10^6 m^{-1}$. The stagnation pressure is 2.87 bar and the stagnation temperature is $293 \text{ K} \pm 5\%$. Adiabatic model conditions are assumed. The freestream turbulence level, determined with laser Doppler anemometry, is approximately 1.4 percent.

2.2 Model

The experimental setup is a flat plate/24° ramp configuration. The origin of the coordinate system is located at the ramp corner on the line of symmetry of the model (see Fig. 2 and Fig. 3, top). The plate is 1265 mm in length with a sharp leading edge. At $x = -70 \text{ mm}$ the thickness of the fully developed turbulent boundary layer is 13.2 mm. The boundary layer transition is calculated to occur close behind the leading edge, say at $x = -1250 \text{ mm}$. Attached to the flat plate is the inclined (24 degree) ramp which has a length of 90 mm. The width of the model is 300 mm, being mounted at the vertical wind tunnel walls.

3 Laser Doppler anemometry

3.1 Limitations and advantages of laser Doppler anemometer (LDA)

LDA is a quantitative, non intrusive measurement technique, thus leaving the flow essentially undisturbed.

As common to most quantifying measurement techniques, the flow can be probed at distinct points only. After collecting a sufficiently large number of samples, a mean value will be calculated.

To plot boundary layer profiles or streamlines of two or three dimensional flows, the fineness of the test grid is crucial.

Obviously the LDA technique cannot simultaneously acquire data at several points. Nevertheless punctual and not time-correlated data can give an important time averaged insight of flow parameters, position and extension of singularities.

3.2 Laser Doppler anemometer at TWM

At the TWM a DANTEC-based 2d-LDA was accomplished. Light source is a COHERENT INNOVA 300-306 6 Watt Argon-ion laser. The two lines of highest intensity, 514.5 (green) and 488 nm (blue) are splitted in a DANTEC high power transmitter box. Combining a 55X82 translater module with a 55X12 beam expander and a focussing lens of 1200 mm produces a measurement volume, the diameter of which is 150 microns. The system is operated in forward scatter mode to derive benefit of the higher scatter intensity.

The measured signals are processed by a 57N10 and a 57N20 ENHANCED DANTEC Burst Spectrum Analyzer. Both velocity components are shifted by 40 MHz. A more detailed description of the LDA-system can be found in [6].

The seeding of the flow is accomplished with a Palas AGF 5.0D atomizer, generating particles with an average diameter of 0.8 μm .

The seeding material is DEHS (Di-2-Ethylhexyl-Sebacate), injected downstream of the pressure control valve, where the air enters the settling chamber.

3.3 Single point measurement

Usually a local LDA measurement is terminated if either a predefined number of particles has passed the volume of measurement or a given sampling time is reached. At the TWM these two parameters are selected to 2000 bursts and 2 seconds, respectively. The velocities u_i of N particles are averaged to give the mean velocity at the point of measurement:

$$u_{mean} = \sum_{i=1}^N \frac{u_i}{N}$$

Similarly the standard deviation is derived:

$$u_{rms} = \frac{\sum_{i=1}^N \sqrt{(u_i - u_{mean})^2}}{N}$$

The separated shock/boundary-layer interaction is well known as a strongly unsteady phenomenon. To derive information about frequencies a sampling rate at least twice as high as the frequency to detect is mandatory. This requirement usually cannot be satisfied by laser Doppler anemometry because of the relatively low data rates.

Best condition to get representative time averaged results is a long sampling time, here 2 seconds. The lowest number of bursts at TWM was about 100. Therefore the data should give a good time averaged image of the investigated flow.

3.4 Multiple point measurements

As laser Doppler anemometry does not allow simultaneous measurements at several points, a time correlation is not possible

To get correlated data, one LDA system per measurement point would be necessary. The first LDA, called master, has to trigger the remaining ones, called slaves. Though simple in theory, the approximately linear rise of costs with each additional LDA will rapidly exceed any realistic scope.

But even if budget would not be crucial (it will !), an extremely high data rate is required. If the master LDA detects a burst, at least one particle must cross the measurement volume of each slave-LDA. To simultaneously detect a sufficiently large number of bursts, the sampling time has to be increased significantly, probably coming in conflict with the limited operating time of a blow down wind tunnel.

Nevertheless the potential of laser Doppler anemometry is used here to get more detailed and more accurate information about the separated flow field. In other words, it is hoped, that

the average location of separation and reattachment, of the shear layer and the shock system will be determined with more accuracy.

3.5 Streamlines

Using the local time averaged velocities u_{mean} and w_{mean} , two dimensional streamlines can be calculated.

The quality of the calculated streamlines depends on the test grid which should be as dense as possible. In unsteady flows, the sampling time emerges as a further parameter to take account of. If, for example, the oscillation of the flow field is about 2 Hz, a poor data rate, say 2 bursts per second, along with sampling time of 1 second is futile. Obviously the sampling time must be long enough to guarantee a sufficient number of bursts for statistical purposes.

Using simple mathematical tools to get the streamlines, fluid mechanical laws may not be taken into account, topological rules may be violated eventually. A shear layer, separating regions with opposite flow, may serve as an example. Assuming zero friction conditions, a line can be found along which the velocity is zero. Presence of friction will give vortices, which are characteristic for shear layers. If a measurement point is located “in the center” of such a layer, the signs of the detected velocities u_{mean} and w_{mean} are accidental. Consequently calculating the streamlines will give results which do not agree with topological considerations.

The direction of streamlines at the boundaries of measurement grids must be carefully interpreted, too. Keeping in mind, that even near surface measurements take place at a finite distance, a small region without data remains. This can lead to erroneous “results”, for example streamlines seemingly pointing normal to surfaces.

4 Experimental results

4.1 Test grid

Laser Doppler anemometry takes information at individual points. Therefore the resolu-

tion – or the number of test points per unit area – is crucially affecting the quality and time of measurement.

Because the measurement time is composed of acquisition time and traversing time, the distance between test points should be kept short. Hence traversing along either the horizontal or vertical axis of the traversing mechanism is a good strategy, resulting in rectangular test grids.

4.2 Global description of the flow field

An overview of the flow field is given in Fig. 3. On top a schlieren picture is depicted. The downstream end of the flat plate and the 24 degree ramp are visible. On the photograph the shock is not represented by a sharp line. As the exposure time was 1/500000 s, dynamic effects can be excluded. Hence the apparent unsharpness will be caused by spanwise effects and by the side wall boundary layer.

In addition to the photograph two results of laser Doppler anemometry are presented. The picture in the center of Fig. 3 shows a contour plot of the time averaged absolute velocity $v_{\text{abs}} = \sqrt{u_{\text{mean}}^2 + w_{\text{mean}}^2}$. According to the Mach number of 2.5 the free stream velocity is about 576 m/s.

The lower picture gives the angle α between the streamlines and the flat plate. Obviously the first deflection of the flow can be determined at an average coordinate of $x = -54$ mm. According to pressure measurements this is 3 mm downstream of X_0 ($x = -57$ mm), compare Fig. 1.

4.3 Boundary layer profiles

In Fig. 4 u_{mean} -curves across the boundary layer are presented for different x -stations. Between $x = -50$ and $x = -34$ mm u_{mean} is positive. At $x = -32$ mm a significant change of the profiles is found, indicating the (time averaged) upstream end of the area of recirculation. The region with negative velocities u_{mean} ends above the ramp at $x = 10$ mm.

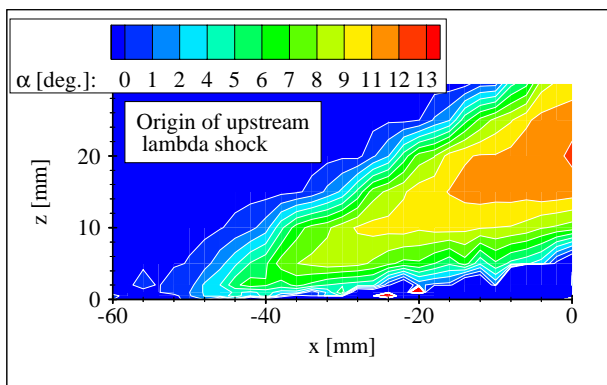
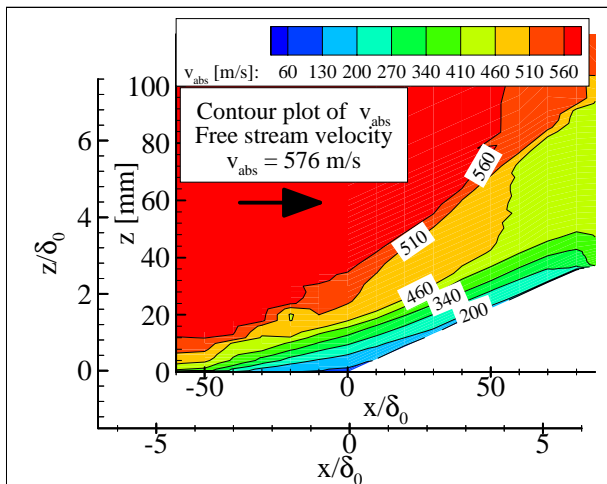
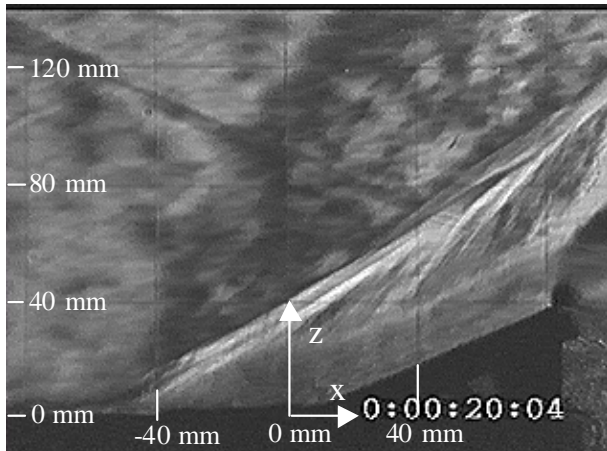


Fig. 3 From top to bottom:
 Schlieren photo;
 Contour plot of absolute velocity;
 Contour plot of shock foot, α : angle of streamlines

$$M = 2.5, Re = 29 \cdot 10^6 m^{-1}$$

Fig. 4, bottom, zooms out the details. The velocity profiles at $x = -36$ and $x = -34$ mm indicate positive values only. At $x = -32$ mm the beginning of upstream (negative) velocity components is detected. At $x = -6$ mm the highest negative value, $u_{mean} = -70$ m/s, is found. The average location of the shear layer is marked with circles. As the layer divides the downstream and upstream pointing portion of the flow, the time averaged velocities u_{mean} and w_{mean} come to zero there.

When drawing the line for $u_{mean} = 0$ m/s as a function of x/δ_0 and z/δ_0 the time averaged angle between shear layer and flat plate can be calculated, which is 4.87 degrees.

As the angle of the upstream λ -shock is 32.8 degrees, a virtual ramp angle of 10 degrees is calculated. This is in accordance with literature [4], where the flow turning angle at separation was reported to be “typically in the order of 5-10 deg., irrespective of ramp angle”.

4.4 Measurements parallel to the model surface

The point of separation is characterized by a change of sign of u_{mean} when traversing in close proximity to the model in streamwise direction. As the measurements must be performed as close as possible to the surface, best parallelity between model and traversing path is desired. At the TWM the angular difference is 0.114 ± 0.014 degrees. For the present investigations, the typical traversing length is 15 mm during one test run, resulting in a z -offset of 0.03 mm. This small value is large enough to enforce permanent adjustment of the LDA-system.

The closest-to-surface measurements along the flat plate could be performed keeping up a distance z_{min} of less than 0.05 mm. For measurements along the ramp, the closest to wall distance had to be increased due to reflections of the laser beams (note that the z -coordinate points normal to the flat plate in any case). In the present study $z = z_{min} + 0.2$ mm could be realized.

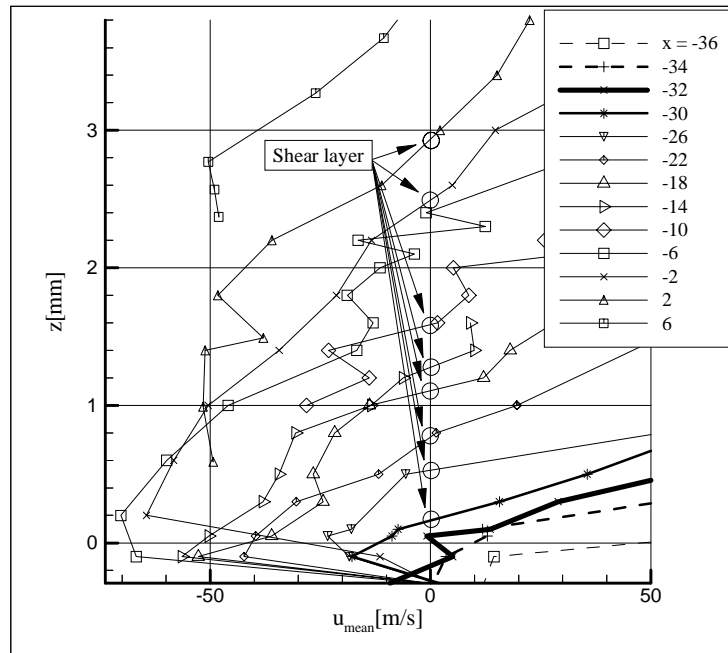
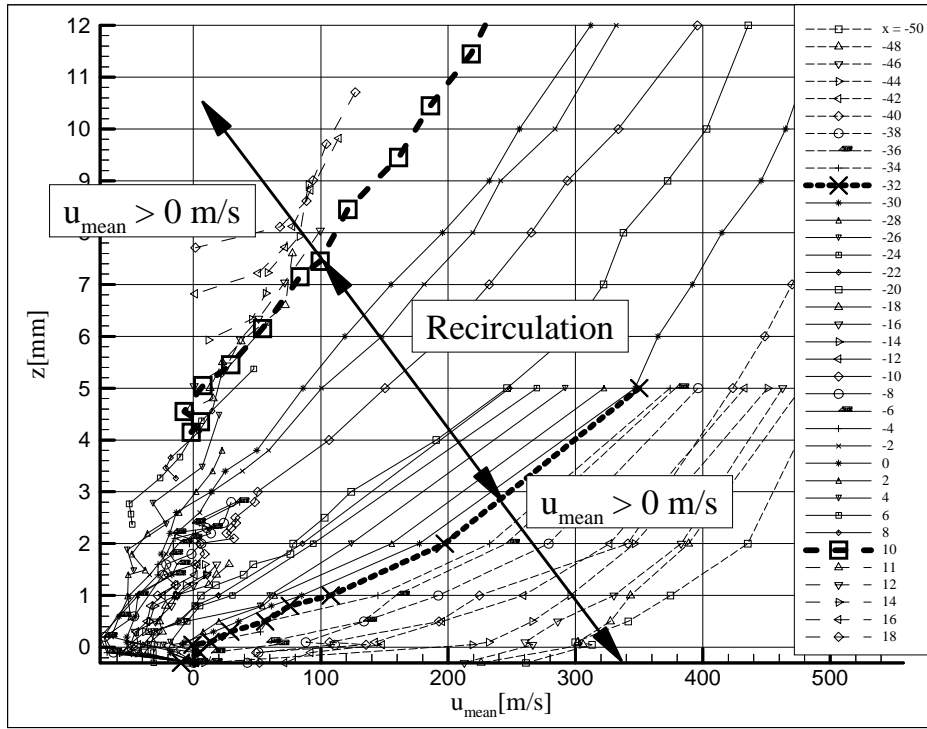


Fig. 4 Boundary layer profiles, bottom: zoom of picture on top

Further optimization of this value by change of the geometrical set up of the LDA system was rejected here for sake of constant parameters.

Velocity profiles of u_{mean} and w_{mean} are plotted as a function of x/δ_0 at three different z-coordinates (see Fig. 5, top). In the region be-

tween S and R, the negative values of u_{mean} indicate the flow reversal. Data of w_{mean} show no significant trend upstream of the ramp corner. At $x/\delta_0 = 0$ a sudden change to negative values occurs, due to the upstream pointing flow along the 24 deg. ramp.

To get representative curves, a polynomial fit of 10th order is used (see Fig. 5, bottom). The time averaged coordinate, where u_{mean} (closest to the surface) changes its sign, can be

determined to be $x/\delta_0 \approx -2.47$. This coordinate is designated by an “S” (incipient separation).

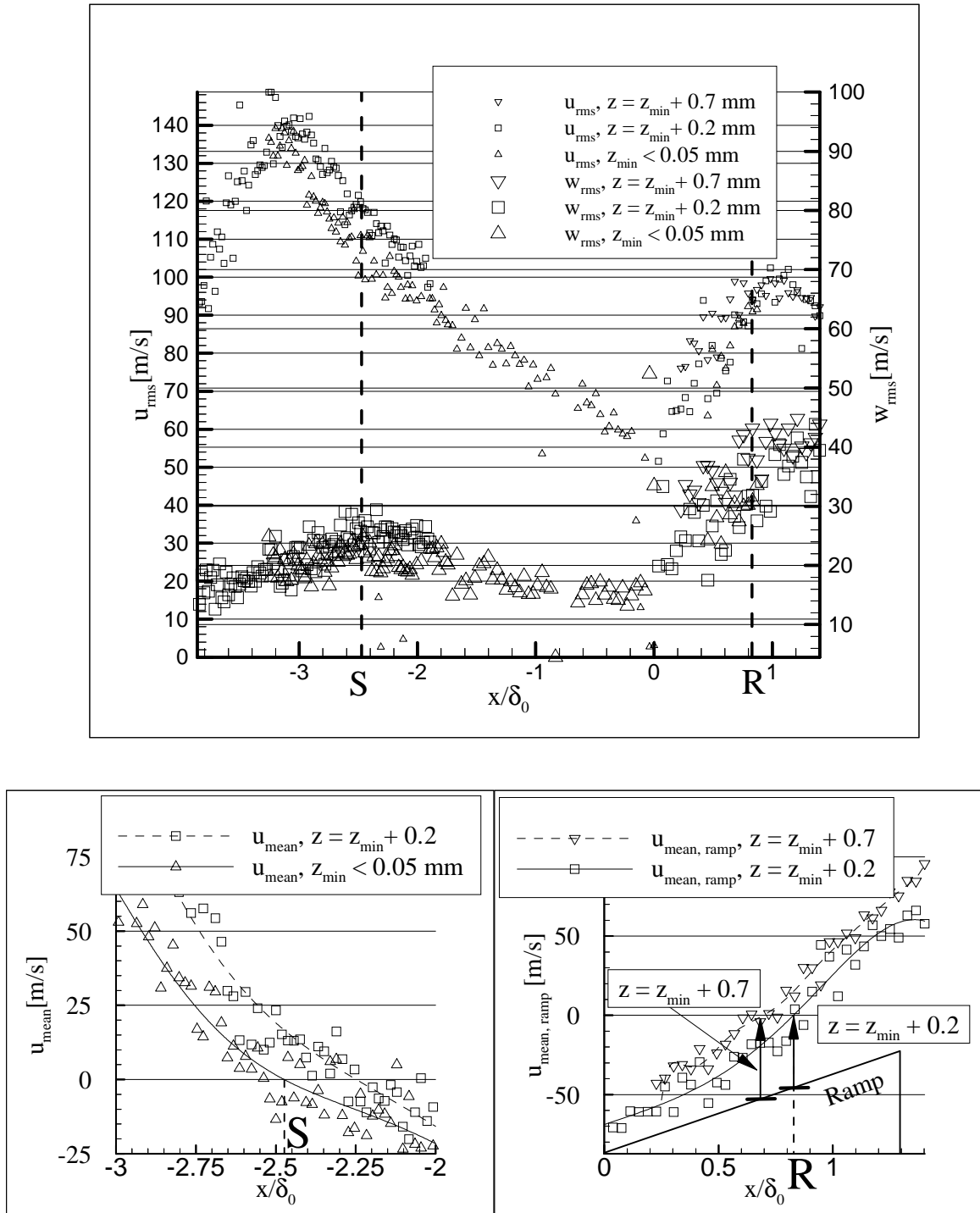


Fig. 5 Top: u_{mean} and w_{mean} velocity profiles close to the surface, $M = 2.5$, $Re = 29 \cdot 10^6 \text{m}^{-1}$
 Bottom: Polynomial fit at point of separation and reattachment

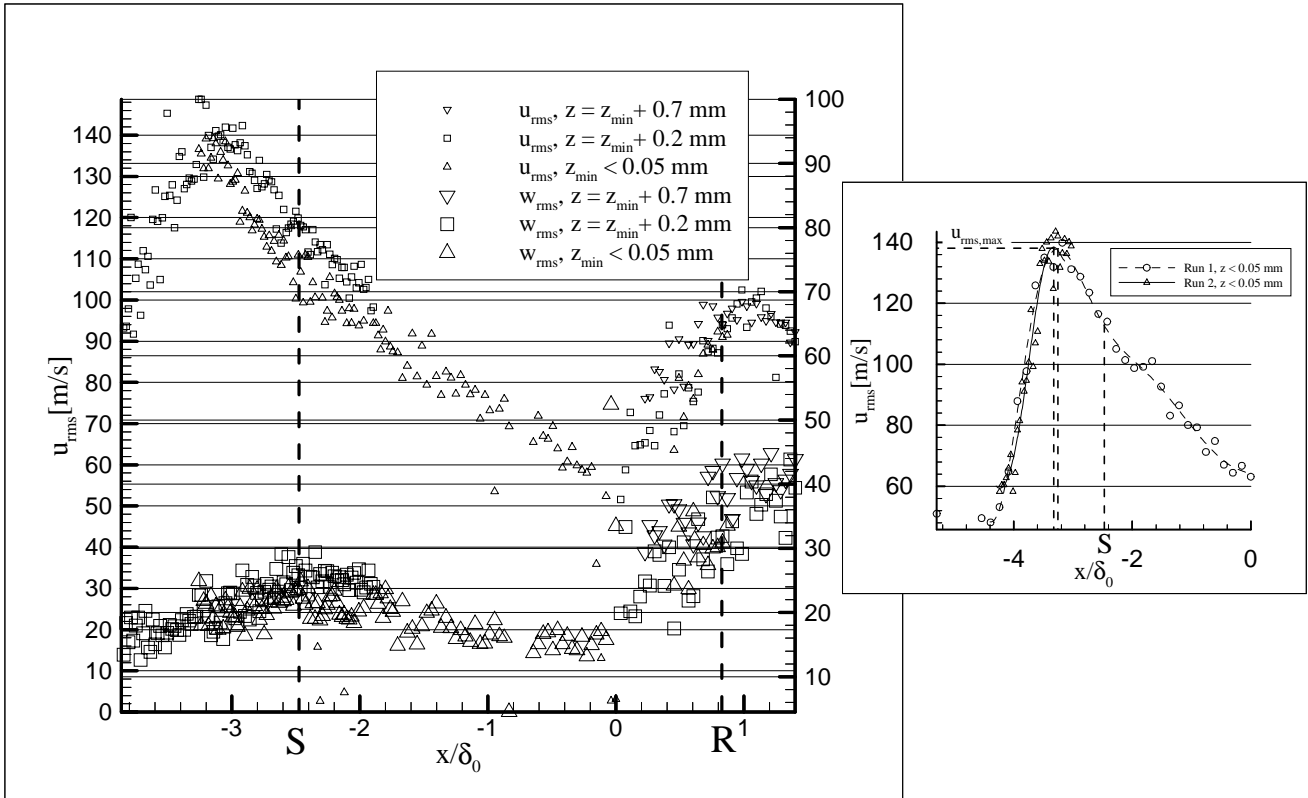


Fig. 6 Standard deviation

The technique to detect the location of reattachment is the same as for separation. The only difference is that the change of sign of the velocity parallel (and as close as possible) to the ramp has to be found now. The z -direction on the ramp is again normal to the x -coordinate, but $z = 0$ is defined at the ramp surface as shown in Fig. 5, bottom, right picture. Again z_{min} is less than 0.05 mm but due to the reflections of the laser beams acceptable data were obtained first at $z = z_{min} + 0.2$ mm, as already stated above. The polynomial fit shows the location of reattachment to be found at $x/\delta_0 = 0.83$.

Both graphs include a curve for a second z -value. At ‘‘R’’ a Δz of 0.5 mm corresponds with a shift of the $u_{mean, ramp} = 0$ m/s – coordinate of $0.15 \cdot \delta_0$. For ‘‘S’’ a Δz of 0.15 mm results in a shift of $0.22 \cdot \delta_0$. Obviously the sensitivity of the measurement in respect to the z -distance is much higher at the location of separation, with its significantly higher gradient,

$$\frac{\partial u_{mean}}{\partial z} > \frac{\partial u_{mean, ramp}}{\partial z}.$$

Pressure measurements [11], [5], revealed that there are two local maxima in the rms distributions: one just ahead of the separation and the other in the vicinity of reattachment. The two rms peaks are confirmed by the u_{rms} curves, see Fig. 6. The maximum upstream of S ($x/\delta_0 = -3.3$) is approximately 140 m/s, nearly three times as high as the free stream value of about 50 m/s. Near R the local maximum is about 100 m/s.

The standard deviation in z -direction w_{rms} does not follow this trend (Fig. 6). The second local maximum is again downstream of R, the first local maximum appears in the vicinity of S, hence downstream of the maximum of u_{rms} .

The free stream level w_{rms} is between 10 and 15 m/s. At S, a level of about 30 m/s is detected. The second maximum (about 60 m/s) is

significantly higher. This observation is opposite to those for u_{rms} .

In [3], the first maximum of the standard deviation of pressures is reported to be “approximately midway between X_0 and S ”. Recalling the results of laser Doppler anemometry and pressure measurements at TWM, the coordinates (x/δ_0) are as follows:

for separation S :	-2.47
for maximum u_{rms} :	-3.3
for X_0 :	-4.32,

thus confirming the trends, [3].

4.5 Area of recirculation

Due to the flexibility of laser Doppler anemometry the flow field can be probed with high resolution. Hence it is possible to derive a contour plot, representing a time averaged picture of the basically unsteady flow field.

Fig. 7, top, shows a contour plot of the absolute velocity, calculated streamlines are superimposed. The area with $v_{\text{abs}} \approx 0$ m/s (\approx shear layer) extends from “ S ” and ends in the vicinity of “ R ”. The streamlines show the expected reverse flow. As mentioned above, no dividing streamline as typical for two dimensional separation (see Fig. 1) is present.

Comparing the distributions of u_{rms} and w_{rms} , two completely different results are obtained. The reported pressure fluctuations between X_0 and S are reflected in the u_{rms} plot whereas the w_{rms} distribution is not affected. Obviously only streamwise flow parameters are influenced by the (longitudinal) oscillation of the shock.

5 Conclusions

The laser Doppler anemometer proved to be a valuable tool for investigations of the separated shock/boundary layer interaction. In addition to conventional pressure measurements a time averaged two dimensional information is obtained not only close to surface but at any point of the flow field.

The points of separation and reattachment are found at the near-wall coordinate where the

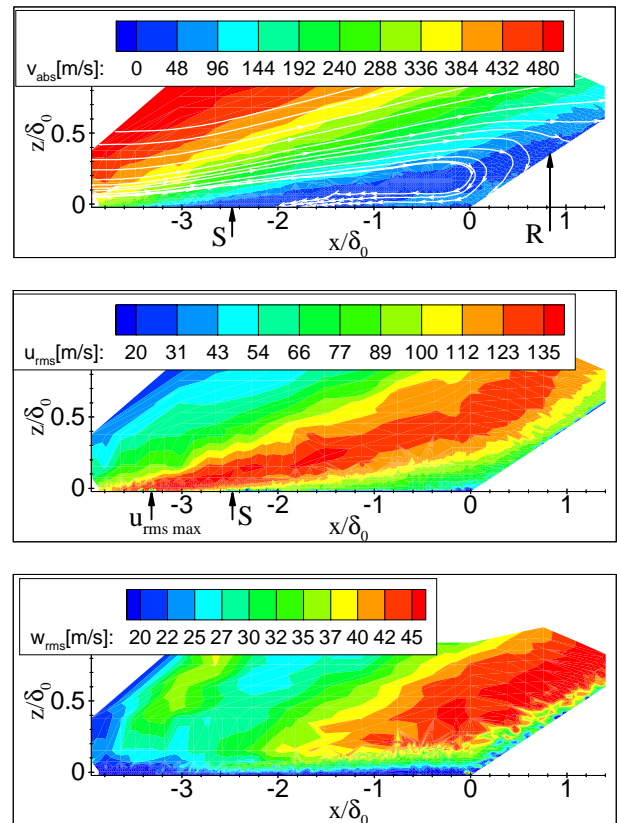


Fig. 7 Contour plots, $M=2.5$, $Re = 29 \cdot 10^6 \text{m}^{-1}$

velocity parallel to the model surface changes its sign.

The results confirm standard deviation peaks at separation and attachment location. Both standard deviations, u_{rms} and w_{rms} , show an maximum increase by a factor of four. At the start of separation the u_{rms} peak is well pronounced. This is reflected by the two dimensional contour plot, too. Obviously the longitudinal oscillation of the shock mainly affects the streamwise flow components.

Future work will investigate the three dimensional flow near the wind tunnel side walls by means of laser Doppler anemometry. In the frame of collaborative research center SFB 255 numerical analysis work is going on to validate turbulence/flow models with the aid of the LDA data base reported here.

Acknowledgement

The authors would like to thank Deutsche Forschungsgemeinschaft (DFG) for supporting

this investigation in the frame of research efforts sponsored in the collaborative research center SFB 255, “Transatmosphärische Flugsysteme, part A5: Shock/Boundary layer interactions”.

References

- [1] Delery J.M. Shock wave boundary layer interaction and its control. *Prog. Aerospace Sciences*, Vol. 22, pp 209-280, 1985.
- [2] Dolling D.S., Murphy M.T. Unsteadiness of the separation shock wave structure in a supersonic compression ramp flowfield. *AIAA Journal*, Vol. 21, No. 12, pp 24-32, 1983.
- [3] Dolling D.S., Or C.T. Unsteadiness of the shock wave structure in attached and separated compression ramp flows. *Experiments in Fluids*, 3,24-32, 1985.
- [4] Dolling D.S. Unsteady phenomena in shock wave/boundary layer interaction. *AGARD-Report* 792, 1993.
- [5] Gramann R.A. *Dynamics of separation and reattachment in a Mach 5 unswept compression ramp flow*. Ph.D. Dissertation, Dept. of Aerospace Engineering and Engineering Mechanics, The Univ. of Texas at Austin, Dec 1989.
- [6] Heiser W. *Experimentelle Untersuchungen von supersonischen Stoß-Grenzschicht-Wechselwirkungen mit Hilfe der Laser-Doppler-Anemometrie*. Dissertation, Institut für Luftfahrttechnik und Leichtbau, Universität der Bundeswehr, München, 1992.
- [7] Marshall A. *An experimental investigation of the spanwise structure of the unsteady separation shock in a Mach 5 unswept compression ramp interaction*. M.S. Thesis, Dept. of Aerospace Engineering and Engineering Mechanics, The Univ. of Texas at Austin, May 1989.
- [8] Marshall T.A., Dolling D.S. Spanwise properties of the unsteady separation shock in a Mach 5 unswept compression ramp interaction. *AIAA Paper*, 90-0377, 28th Aerospace Sciences Meeting, Reno, NV, 1990.
- [9] Marshall A., Dolling D.S. Comments on the computation of supersonic, unswept, turbulent compression ramp interactions, *AIAA Journal*, Vol. 30, No. 8, pp. 2056-2065, Aug. 1992.
- [10] Müller J. *Experimentelle Grundlagenuntersuchungen von supersonischen Rezirkulationsphänomenen an einer Rampenkonfiguration*. Dissertation, Institut für Luftfahrttechnik, Universität der Bundeswehr München, Shaker Verlag, 1998.
- [11] Murphy M. *An experimental investigation of the separation shock wave unsteadiness in a compression ramp flowfield*. M.S.E. Thesis 1605-T, Mechanical and Aerospace Engineering Dept., Princeton University, 1983.
- [12] Nordyke R.J. *Spanwise properties of the unsteady separation in a Mach 5 unswept compression ramp interaction*. M.S. Thesis, Dept. Of Aerospace Engineering Mechanics, The University of Texas at Austin, May 1987.
- [13] Price A.E., Stallings R.L. Investigation of turbulent separated flows in the vicinity of fin type protuberances at supersonic Mach numbers. *NASA TN D-3840*, 1967.